International Immunopharmacology 74 (2019) 105713

Contents lists available at ScienceDirect

International Immunopharmacology

journal homepage: www.elsevier.com/locate/intimp

GSDMD is required for effector CD8$^+$ T cell responses to lung cancer cells

Guangmin Xi[a,b,*], Jianwei Gao[a,c], Bing Wan[a,c], Ping Zhan[a,c], Wujian Xu[a,c], Tangfeng Lv[a,c], Yong Song[a,c,*]

[a] Department of Respiratory Medicine, Jinling Hospital, Nanjing University School of Medicine, Nanjing 210002, China
[b] College of Life Science, Qi Lu Normal University, Jinan, Shandong 250012, China
[c] Nanjing University Institute of Respiratory Medicine, Nanjing 210002, China

ARTICLE INFO

Keywords:
Gasdermin family
GSDMD
CTL
Immune response
NSCLC

ABSTRACT

GSDMD is a recently discovered pyroptosis executioner in monocytes whose N-terminal domain can insert into the inner leaflet of cell membranes and form extensive pores. However, the function of GSDMD in other biological systems remains unclear. In this study, we showed that the expression of GSDMD was consistently correlated with CD8$^+$ T cell markers in The Cancer Genome Atlas (TCGA) cohorts. GSDMD cleavage increased in OT-1 cytotoxic T lymphocytes (CTLs) and human activated CD8$^+$ T cells. Colocalization of GSDMD with granzyme B was observed in the proximity of immune synapses, and GSDMD deficiency reduced the cytolytic capacity of CD8$^+$ T cells. Overall, our study highlights a function, to our knowledge previously unknown, for GSDMD in CTLs and demonstrated that GSDMD is required for an optimal CTL response to cancer cells.

1. Introduction

Cytotoxic T lymphocytes (CTLs) play a critical role in protection against intracellular pathogens and tumors. To induce target cell death, CTLs mainly use two major contact-dependent cytotoxic pathways that are dependent on the Fas ligand and lytic granules [1]. CTLs principally eliminate malignantly transformed cells by releasing the contents of cytotoxic granules into the immune synapse formed with the target cell [2]. Granule serine proteases, known as granzymes (Gzms), induce apoptosis after they are delivered into the target cell cytoplasm by the pore-forming granule protein perforin [3,4].

Thus far, apoptosis has been the most accepted form of target cell death because it does not induce inflammatory responses and avoids damage to neighboring bystander cells [5–9]. However, target cells are killed quickly by cytolysis, as evidenced by the release of cell contents. The ^{51}chromium-release assay is the most commonly used and has been the gold standard for measuring CTL cytotoxicity *in vitro* [10–12]. In this assay, cell death was determined by measuring the amount of chromium-51 bound to proteins in the supernatant, which indicates that the integrity of target cell membranes are disrupted during CTL attack [10,13]. In the previous studies, the only reported pore-forming protein used by CD8$^+$ T cells is perforin [14]. Perforin can form pores on the target cell membrane to enable granzymes and granulysin to diffuse into target cell cytosol directly or form pores on the endosomes to deliver granzymes into the cytosol indirectly [15]. However, the function of perforin seems to be limited to the entrance of granzymes into the target cell in the models mentioned above [16]. Moreover, the perforin pores are restricted to the confined area of an immune synapse, and recent studies have shown that perforin pores on the target cell plasma membrane are transient because of a wound repair response triggered by pores on the target membrane [17,18]. Therefore, we hypothesize that other pore-forming proteins, particularly those that can form pores from within mammalian cells, are implicated in the target cell killing process of CTL. Because GSDMD is a recently discovered pore-forming protein whose N-terminal domain can insert into the inner leaflet of cell membranes and form extensive pores [19], we speculate that GSDMD participates in the CTL attack process.

GSDMD belongs to the gasdermin (GSDM) family that is conserved in vertebrates and comprises six paralogs in humans: GSDMA, GSDMB, GSDMC, GSDMD, DFNA5 and DFNB59. Mice lack Gsdmb and have three GSDMDA homologs, four GSDMC homologs, GSDMD, DFNA5, and DFNB59. Proteins of the GSDM family are mainly expressed in epithelial tissues and play a role in the regulation of cell proliferation and/or differentiation [20]. Recent discoveries showed that GSDMD is the key executioner of pyroptosis [21,22]. Pyroptosis is a pro-inflammatory form of programmed necrosis, which is characterized by the early permeabilization of the plasma membrane and release of pro-inflammatory cytokines [21].

GSDMD contains 484 amino acids divided into two domains, the N- and C-terminal domains that are linked by an interdomain [22]. When

* Corresponding authors at: Department of Respiratory Medicine, Jinling Hospital, Nanjing University, #305, East Zhongshan Road, Nanjing 210002, China.
E-mail addresses: 475810355@qq.com (G. Xi), yong_song6310@yahoo.com (Y. Song).

https://doi.org/10.1016/j.intimp.2019.105713
Received 26 April 2019; Received in revised form 15 June 2019; Accepted 18 June 2019
Available online 02 July 2019

pyroptosis is induced, activated caspase-1 and caspase-11 (caspase-4/5) efficiently cleave GSDMD at the conserved residue D276 within the interdomain, which separates GSDMD into a GSDMD-N domain and a GSDMD-C domain [22,23]. Consequently, the GSDMD-N domain partitions to cellular membranes and forms extensive pores on the plasma membrane [19,24]. The pores mostly have an inner diameter of 12–14 nm, with approximately 16 symmetric protomers. Thus, GSDMD is a pore-forming protein that normally exists in an auto-inhibited state. Different from known pore-forming proteins, GSDMD can only cause cell lysis from within mammalian cells because of the asymmetric distribution of phosphoinositides on the plasma membrane [19]. The formation of membrane pores by GSDMD disrupts the osmotic potential, causing cell lysis and release of pro-inflammatory cytokines. Although the role of GSDMD in pyroptosis is clear, the function of GSDMD in other biological system remains unclear. In the present study, we investigated the role of GSDMD during CTL responses to NSCLC cells.

2. Materials and methods

2.1. Cell lines

3LL and NCI-H1299 cell lines were obtained from the Cell Bank of the Chinese Academy of Science (Shanghai, China). 3LL and H1299 cells were cultured in RPMI-1640 medium (HyClone, USA) supplemented with 10% FBS (HyClone), 100 IU/ml penicillin, and 100 mg/ml streptomycin. 3LL-OVA cells were generated by transfection with a lentiviral plasmid harboring cytosolic chicken ovalbumin.

2.2. Mice

Female wild-type C57BL/6 mice and TCR-transgenic OT-1 mice (8–10 weeks old) were purchased from the Model Animal Research Center of Nanjing University (Nanjing, China). Housing and all experimental animal procedures were approved by the Institutional Animal Care and Use Committee of the Jinling hospital, Nanjing University.

2.3. Mouse $CD8^+$ T cell isolation and stimulation

Primary mouse T cells were isolated from spleens using Histopaque (Sigma, USA) and cultured *in vitro* in RPMI-1640 medium supplemented with 10% FBS. To generate mature CTLs, splenocytes isolated from OT-1 mice were stimulated with 10 ng/ml $OVA_{257–264}$ for 3 days in the presence of 100 IU/ml IL-2. Cells were centrifuged and cultured in fresh medium containing 100 IU/ml of IL-2 for 2 more days, after which most of the cells in the culture were CTLs [25]. T cell enrichment was performed with $CD8^+$ T Cell Isolation Kit (Miltenyi Biotec).

2.4. Human $CD8^+$ T cell isolation and stimulation

Peripheral blood mononuclear cells (PBMCs) were isolated from the blood of patients with lung adenocarcinoma (LUAD). Blood samples were collected and processed after obtaining written informed consent from each donor and approval for this study by the local ethics committee. PBMCs were stimulated with 5 μg/ml of soluble anti-CD3/anti-CD28 (ebioscience) in RPMI 1640 medium supplemented with 10% FBS and 100 IU/ml of IL-2 for 7 days. $CD8^+$ T cells were then purified using the $CD8^+$ T Cell Isolation Kit (Miltenyi Biotec), according to the manufacturer's instructions.

2.5. Real-time PCR analysis

Total RNA was extracted using the TRIzol reagent (TaKaRa), according to the manufacturer's protocol. Total RNA (1 μg) was used as a template to synthesize cDNA with M-MLV Reverse Transcriptase (Takara). Real-time PCR was performed using SYBR Premix Ex Taq (TaKaRa) in a 20 μl reaction system, following the manufacturer's instructions. The PCR conditions were as follows: enzyme activation at 95 °C for 10 s, followed by 40 cycles of denaturing at 95 °C for 10 s and extension at 60 °C for 34 s. All assays were performed in triplicate. Results were normalized to the expression level of β-actin. Primers sequences are provided in Supplementary Tables S1, S2.

2.6. Western blot analysis

Cells were washed twice with PBS and lysed with SDS sample buffer. After centrifugation (12,000 *g*, 20 min), supernatants were collected. Identical amounts of cell lysates were separated by 12% SDS-PAGE and electrophoretically transferred onto polyvinylidene fluoride membranes. After being blocked with 5% fat-free milk for 1 h at room temperature, the membranes were immunoblotted with perforin-1 (Santacruz, sc-373943), interferon-γ (Abcam, ab9657), granzyme B (Santacruz, sc-8022), GSDMD (Santacruz, sc-81868), GSDMD (Abcam, ab209845), GSDMD (Abcam, ab155233), Caspase-1 (CST, #2225), Caspase-11 (CST, #14340), Caspase-4 (CST, #4450), Caspase-5 (CST, #46680) and β-actin (CST, #3700) overnight. Subsequently, membranes were washed three times, incubated with HRP-conjugated secondary antibodies for 1 h at room temperature, and washed extensively before detection. Protein bands were visualized using ECL reagent (Beyotime, China) and images were captured with a Gel Doc XRS (Bio-Rad).

2.7. Immunofluorescence cell staining

T cells harvested after stimulation were washed twice with PBS. T cell suspensions were then mounted on slides and dried at room temperature for 2 h to make the cells adhere to the slide. Cells were fixed in 4% paraformaldehyde for 15 min at room temperature, washed in PBS, permeabilized with 0.2% Triton X-100 for 15 min, and blocked for 60 min with PBS containing 5% BSA (w/v). Cells were immunostained with granzymeB (Santacruz, c-8022), GSDMD (Abcam, ab209845) GSDMD (Abcam, ab155233) overnight. After washing three times, the cells were probed with FITC-conjugated goat anti-rabbit-IgG or Alexa Fluor 555-conjugated goat anti-mouse-IgG (Invitrogen) for 1 h at room temperature. Nuclei were counterstained with DAPI. Fluorescent micrographs were obtained using a fluorescence microscope (Zeiss, Oberkochen, Germany).

2.8. Lentiviral vector transduction

Lentiviral vectors encoding GSDMD shRNA were purchased from Gene Pharma Biotechnology Company (Shanghai, China). The designed DNA fragments were cloned into the plasmid pWPXLd. Subsequently, this vector plasmid with packaging plasmids psPAX2 and envelope plasmid pMD2.G co-transfected into packaging cell line (293T) using calcium phosphate method. The constructed viral vector was harvested, purified and concentrated and stored at −80 °C for next experiments. The titration of the vector was carried out using fluorescent microscopy. The sequence of shRNA of GSDMD was supplied in the supplementary data (Table S3). Lentiviral vector was transduced into OT-1 cells after primary peptide stimulation. After 24 h, the medium was replaced with fresh complete medium containing IL-2, and the cells were cultured for another 5 days.

2.9. In vitro cytotoxicity assays

3LL-OVA cells, transfected with cytosolic chicken ovalbumin, were cultured in 96-well plates and allowed to attach by overnight incubation. OT-1 CTLs were added to 3LL-OVA cells at various effector to target ratios and incubated for 4 h at 37 °C in RPMI-1640 medium supplemented with 2% FBS. Target cell death was assayed using the Pierce LDH cytotoxicity assay kit (Thermo Scientific), according to the

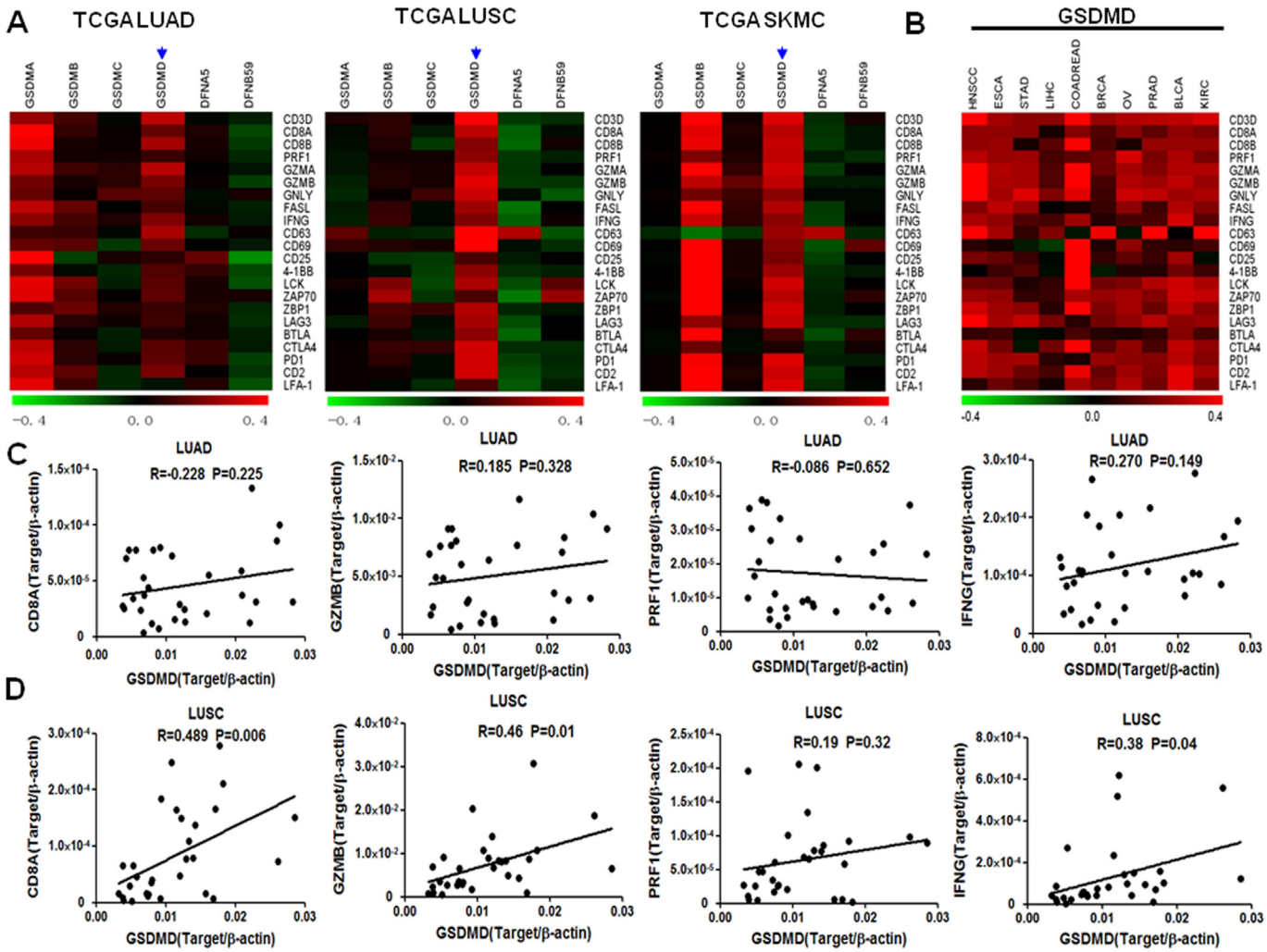

Fig. 1. GSDMD was positively correlated with CD8$^+$ T cell markers in the tumor samples. (A) Heatmaps showing correlation of the genes of the gasdermin family with CD8$^+$ T cell markers in lung adenocarcinoma (LUAD) (n = 522), lung squamous carcinoma (n = 504), and skin melanoma (n = 479) TCGA cohorts. (B) The co-expression between GSDMD and CD8$^+$ T cell markers was analyzed in head and neck squamous cell carcinoma (HNSCC), esophageal carcinoma (ESCA), stomach adenocarcinoma (STAD), liver hepatocellular carcinoma (LIHC), colorectal adenocarcinoma (COADREAD), breast invasive carcinoma (BRCA), ovarian serous cystadenocarcinoma (OV), prostate adenocarcinoma (PRAD), bladder urothelial carcinoma (BLCA), and kidney renal clear cell carcinoma (KIRC). (C) The correlations of GSDMD with CD8A, GZMB, PRF1, and IFNG were analyzed in 30 samples from patients with LUAD who had undergone surgeries at the Jinling hospital. (D) The correlations of GSDMD with CD8A, GZMB, PRF1, and IFNG were analyzed in 30 samples from patients with lung squamous cell carcinoma (LUSC) who had undergone surgeries at the Jinling hospital.

manufacturer's protocol. For CD8$^+$ T cells that were derived from human peripheral blood, T cells were stimulated with soluble anti-CD3/anti-CD28 antibodies (ebioscience, USA) for 7 days and used as effector cells. H1299 cells were used as target cells.

To evaluate the role of GSDMD in T cell cytotoxicity, OT-1 CD8$^+$ T cells were stimulated with $OVA_{257–264}$ and transduced with mock or shGSDMD vector. ShRNA-mediated suppression of GSDMD was routinely confirmed by Western blot. OT-1 CTLs expressing scrambled or shGSDMD were then mixed with 3LL-OVA cells at different effector to target ratios. After 4 h, the cytotoxic efficiency was measured using the Pierce LDH cytotoxicity assay kit (Thermo Scientific).

To evaluate the role of GSDMD in human T cell cytotoxicity, T cells were stimulated and transduced with mock or shGSDMD vector. ShRNA-mediated suppression of GSDMD was routinely confirmed by Western blot. Activated CD8$^+$ T cells expressing scrambled or shGSDMD were mixed with H1299 cells at different effector to target ratios. After 4 h, the cytotoxic efficiency was measured using the Pierce LDH cytotoxicity assay kit (Thermo Scientific).

2.10. Immunohistochemistry

Tumor tissues were harvested from consenting patients and fixed in 10% formalin. After paraffin embedding, tumor specimens were cut into 5 μm sections and placed on slides. Samples were deparaffinized in xylene and rehydrated using a series of graded alcohol. Antigen retrieval was performed by heat treatment in citrate buffer. Samples were blocked with 10% goat serum before incubation with the primary antibody. The samples were incubated overnight in a humidified container at 4 °C using the following primary antibodies: mouse anti-GSDMD (64-Y; 1:200) or an isotype-matched IgG as a negative control. Immunohistochemical staining was performed with the Dako Envision Plus System (Dako, Carpinteria, USA), according to the manufacturer's instructions.

2.11. Bioinformatics analysis

TCGA LUAD data (TCGA provisional, n = 522, http://www.cbioportal.org/), LUSC data (TCGA provisional, n = 504, http://www.cbioportal.org/), and skin cutaneous melanoma data (TCGA

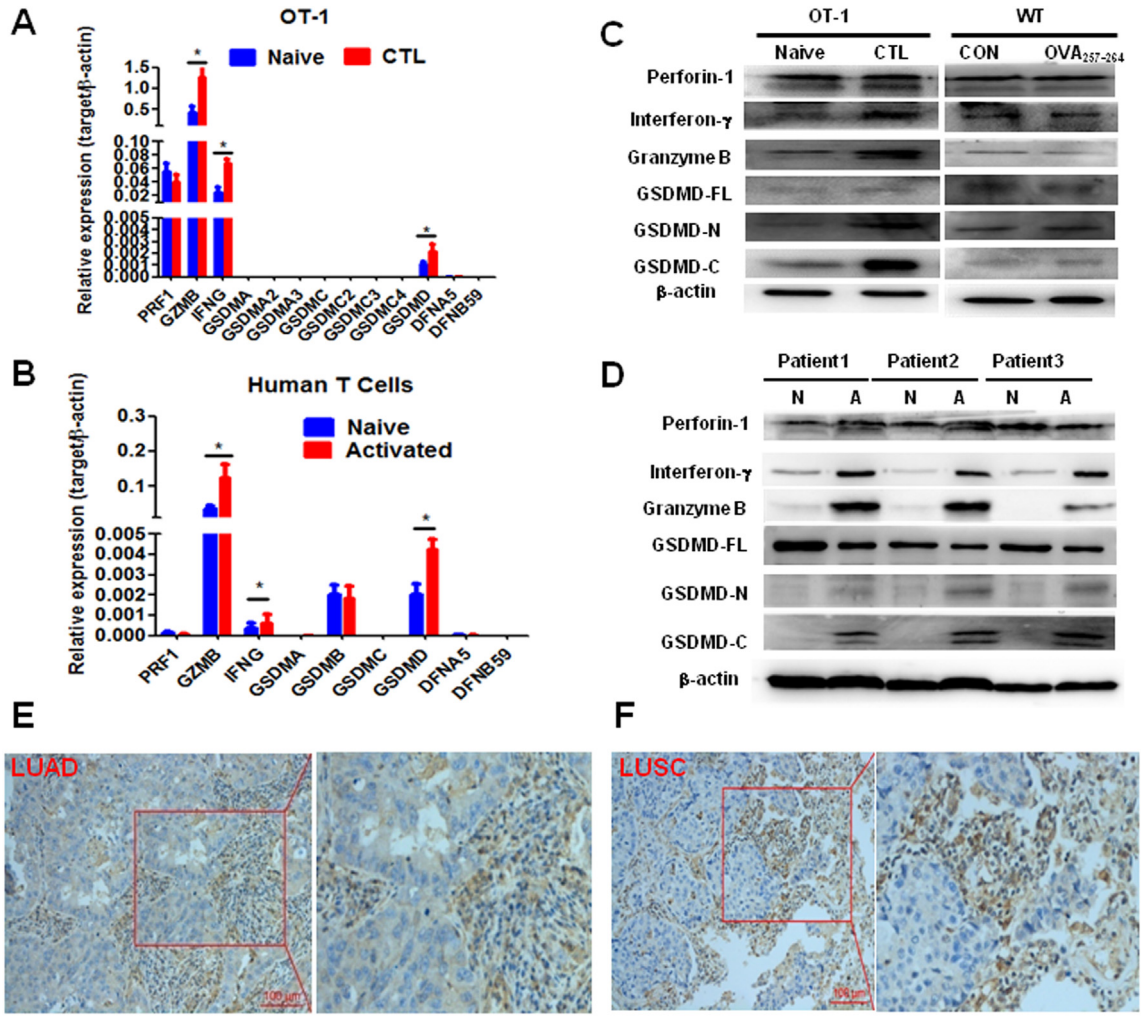

Fig. 2. GSDMD was upregulated in activated $CD8^+$ T lymphocytes. (A) The mRNA expression levels of PRF1, GZMB, IFNG, and the gasdermin family genes in naïve T lymphocytes or CTLs from the OT-1 mouse. Splenocytes from OT-1 mice were stimulated with the $OVA_{257–264}$ peptide for 5 days, after which $CD8^+$ T cells were sorted and the indicated genes were determined by real-time PCR. Results represent the mean ± SD from three experiments; *P < 0.05. (B) The mRNA expression levels of PRF1, GZMB, IFNG, and the gasdermin family genes in naïve or activated $CD8^+$ T cells from patients with lung adenocarcinoma (LUAD). Peripheral blood mononuclear cells (PBMCs) were isolated and stimulated with 5 μg/ml of soluble anti-CD3/anti-CD28, after which $CD8^+$ T cells were sorted by negative selection methods and the indicated genes were determined by real-time PCR. Results represent the mean ± SD from three experiments. (C) The left panel shows the protein expression levels of perforin-1, granzyme B, interferon-γ, and GSDMD in naïve T lymphocytes or CTLs from the OT-1 mouse. The right panel shows the protein expression levels of perforin-1, granzyme B, interferon-γ, and GSDMD in wild-type C57BL/6 $CD8^+$ T cells cultured in the presence or absence of the $OVA_{257–264}$ peptide. (D). Protein expression levels of perforin-1, granzyme B, interferon-γ, and GSDMD in naïve or activated $CD8^+$ T cells from patients with LUAD (N = Naïve and A = Activated). (E) Overview of immunohistochemistry for GSDMD in tumor-infiltrating lymphocytes. Representative GSDMD staining pictures for LUAD are shown. (F) Representative GSDMD staining pictures for LUSC are shown.

provisional, n = 479, http://www.cbioportal.org/) were used to determine the correlation between the expression of gasdermin family genes and $CD8^+$ T cell marker genes. The co-expression of GSDMD and $CD8^+$ T cell markers was further analyzed in other tumor cohorts of TCGA (http://www.cbioportal.org/). The results of Pearson correlation analysis were used to make heatmaps.

2.12. Statistical analysis

The results were expressed as the mean ± SD. Results of expression analyses were evaluated using the two-tailed Student's *t*-test. We used a Pearson correlation to analyze correlations between expressions of genes. A two-sided P value of < 0.05 was considered statistically significant. Statistical analyses were performed with the SPSS 19.0 software.

3. Results

3.1. The expression of GSDMD is positively correlated with $CD8^+$ T cell marker levels in tumor samples

We investigated the associations between the expression of GSDM family genes and $CD8^+$ T cell markers in primary tumors from lung adenocarcinoma (LUAD), lung squamous cell carcinoma (LUSC), and melanoma (SKMC) cohorts from TCGA. The expression of GSDMD, but not other GSDM family genes, showed a consistent positive correlation with $CD8^+$ T cell markers, such as CD8A, CD8B, PRF1, GZMA, GZMB, and IFNG, in LUAD (n = 522, Fig. 1A), LUSC (n = 504, Fig. 1A), and melanoma (n = 479, Fig. 1A) cohorts. To confirm the findings, further analysis was performed in other tumor cohorts (Fig. 1B). Similar positive correlations were observed between GSDMD and $CD8^+$ T cell markers, which confirmed that the association was not restricted to NSCLC and melanoma. The correlations of GSDMD with CD8A, PRF1,

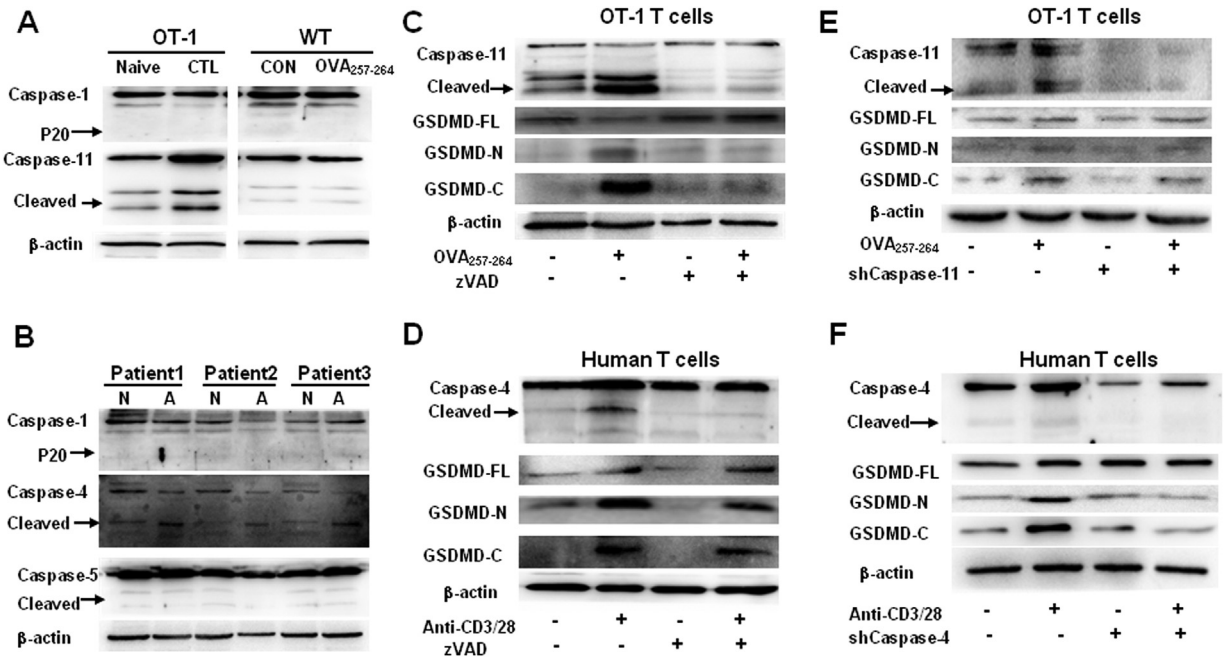

Fig. 3. GSDMD was cleaved by caspase-4/11 in activated CD8$^+$ T cells. (A) The left panel shows the protein expression levels and activation status for caspase-1 and caspase-11 in OT-1 CD8$^+$ T cells cultured in the presence or absence of the $OVA_{257–264}$ peptide. The right panel shows the protein expression levels and activation status for caspase-1 and caspase-11 in wild-type C57BL/6 CD8$^+$ T cells cultured in the presence of absence of the $OVA_{257–264}$ peptide for 5 days. (B) The protein expression level and activation status for caspase-1, -4, and -5 in naïve or activated human CD8$^+$ T cells. (C) The effect of z-VAD-FMK on the expression and activation of GSDMD in activated OT-1 CD8$^+$ T cells. T cells stimulated with the $OVA_{257–264}$ peptide were cultured in the absence or presence of 40 μM z-VAD-FMK. The expression and activation of caspase-11 and GSDMD were measured after 5 days using Western blot. (D) The effect of z-VAD-FMK on the expression and activation of GSDMD in activated human CD8+ T cells. T cells stimulated with soluble anti-CD3/anti-CD28 were cultured in the absence or presence of 40 μM z-VAD-FMK. After 7 days, the expression and activation of caspase-4 and GSDMD were measured using Western blot. (E) The effect of shCaspase-11 on the expression and activation of GSDMD in OT-1 T cells. The expression and activation of caspase-11 and GSDMD were measured using Western blot. (F) The effect of shCaspase-4 on the expression and activation of GSDMD in activated human CD8+ T cells. T cells stimulated with soluble anti-CD3/anti-CD28 were cultured in the absence or presence of shCaspase-4. After 7 days, the expression and activation of caspase-4 and GSDMD were measured using Western blot.

GZMB, and IFNG were further analyzed in 30 samples from patients with NSCLC who had undergone surgeries at the Jinling hospital. We found that GSDMD was positively correlated with CD8A, GZMB, and IFNG in the additional 30 samples of NSCLC, which confirmed the results from TCGA (Fig. 1C, D). We therefore hypothesized that GSDMD is associated with the function of CD8$^+$ T cells.

3.2. GSDMD was up-regulated in activated CD8$^+$ T cells

Mice lack GSDMB has three GSDMA homologs, four GSDMC homologs, DFNA5, and DFNB59 in addition to Gsdmd. GSDM family members have similar molecular structures and share approximately 45% sequence homology. We initially determined the expression pattern of GSDM family genes during the activation of CD8$^+$ T cells by real-time PCR. We found that the expression of GSDMD was the highest among GSDM family genes in activated OT-1 CD8$^+$ T cells (Fig. 2.A). Moreover, compared with naïve T cells, GSDMD mRNA was significantly up-regulated in CTLs activated with the $OVA_{257–264}$ peptide (Fig. 2A).

In humans, the GSDM family genes comprise six paralogs: GSDMA, GSDMB, GSDMC, GSDMD, DFNA5, and DFNB59. To determine the role of the GSDM family in human CD8$^+$ T cells, we assessed gene expression levels for the six GSDM paralogs. Consistent with the results obtained from CTLs of the OT-1 mouse, we found that the expression level of GSDMD was the highest among GSDM family members in activated human CD8$^+$ T cells (Fig. 2B). The expression of GSDMD mRNA was up-regulated following the activation of CD8$^+$ T cells (Fig. 2B). We further tested the expression of the GSDMD protein by Western blot, and the results showed that the expression of GSDMD protein was significantly up-regulated in mouse CTLs, mainly in a cleaved form (Fig. 2C). In addition, the cleaved GSDMD-N and GSDMD-C domains could only be observed in activated human CD8$^+$ T cells (Fig. 2D). Moreover, we detected the expression of the GSDMD protein in NSCLC samples. High expression of GSDMD was observed in tumor-infiltrating lymphocytes in lung adenoma (Fig. 2E) and squamous cell cancers (Fig. 2F).

3.3. GSDMD was cleaved by caspase-4/11 in activated CD8$^+$ T cells

Previous studies demonstrated that GSDMD is specifically cleaved by inflammatory caspases. Inflammatory caspases comprise caspase-1, -4, -5 and 11 [26]. To determine the possible involvement of inflammatory caspases in the cleavage of GSDMD, we assessed the expression and activation state of these caspases in activated CD8$^+$ T cells. Our results showed that the activation of caspase-11 was enhanced in the activated OT-1 CD8$^+$ T cell (Fig. 3A). The activation of the human homolog caspase-4 was also enhanced in the activated CD8$^+$ T cell (Fig. 3B). To further verify the involvement of caspase-4 or -11 in the cleavage of GSDMD, the pan-caspase inhibitor z-VAD-FMK was used to inhibit the activity of caspases. The cleavage of GSDMD was partially blocked by z-VAD-FMK treatment (Fig. 3C, D). Moreover, we employed shRNA targeting capase-11 or caspase-4 for functional studies. Knockdown of capase-11 expression significantly attenuated the cleavage of GSDMD in OT-1 T cells (Fig. 3E). Knockdown of capase-4 expression significantly attenuated the cleavage of GSDMD in Human T cells (Fig. 3F). All these results indicated that GSDMD was cleaved partially *via* activation of caspase-4 or -11. The other unknown mechanism may also be used to cleave GSDMD in activated CD8$^+$ T cells.

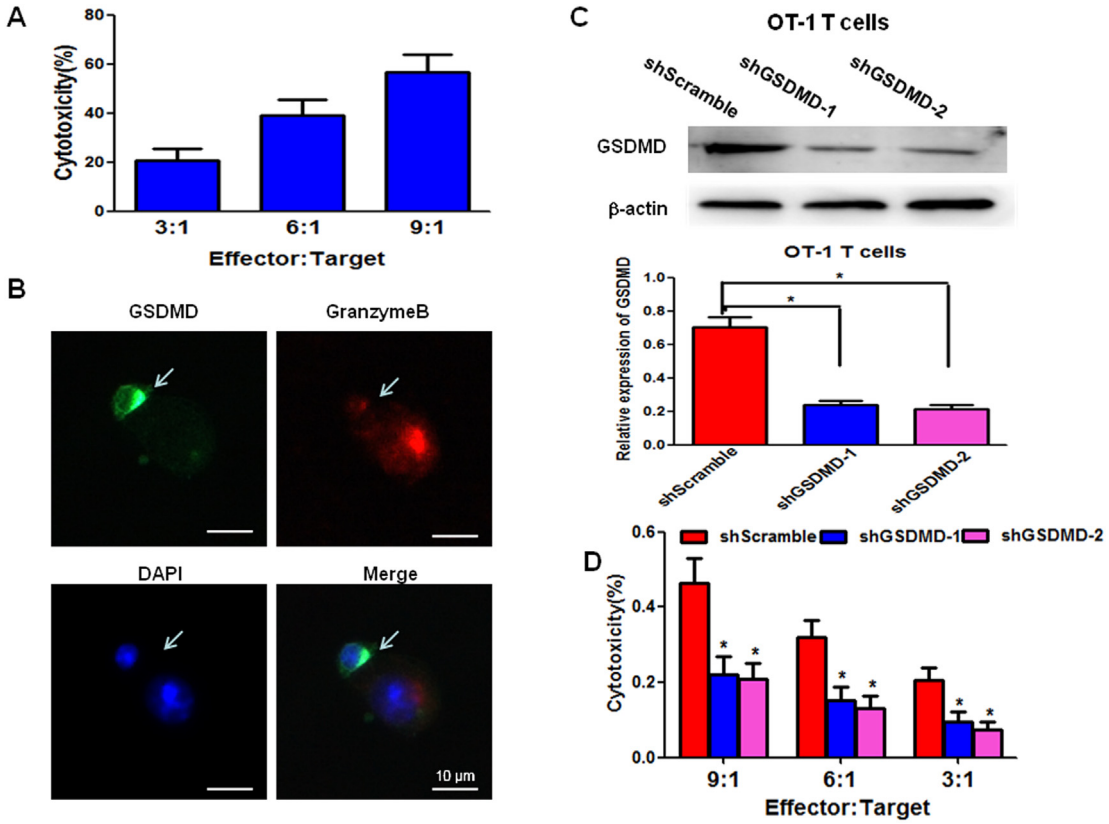

Fig. 4. GSDMD deficiency reduces the cytolytic capacity of OT-1 $CD8^+$ T cells. (A) Activated OT-1 $CD8^+$ T cell cytotoxicity on 3LL-OVA target cells. Splenocytes from OT-1 mice were stimulated with $OVA_{257–264}$ to generate mature CTLs. CTLs were incubated with 3LL-OVA cells for 4 h, after which LDH release was measured to assess cytotoxic efficiency. Data are representative of three independent experiments. (B) Fluorescence microscopy images of OT-1 CTLs conjugated with 3LL-OVA cells. CTLs were mixed with 3LL-OVA cells for 4 h, fixed, and stained for GSDMD and granzymeB to visualize the distribution of GSDMD and granzymeB in CTLs. (C) ShRNA-mediated suppression of GSDMD was routinely confirmed by Western blot. (D) *In vitro* cytotoxic assay for specific lysis of 3LL-OVA target cells by OT-1 CTLs expressing scrambled or GSDMD shRNA. Specific lysis for 4 h is shown at the indicated effector to target ratios. All killing assays were performed in triplicates. *P < 0.05.

3.4. GSDMD deficiency reduces the cytolytic capacity of OT-1 CTLs

To evaluate the contribution of GSDMD in specific CTL cytotoxicity, we initially examined CTL responses of OT-1 T cells to ovalbumin-expressing Lewis lung carcinoma (3LL-OVA) cells. Splenocytes from OT-1 mice were activated with $OVA_{257–264}$ for 5 days, after which $CD8^+$ T cells were sorted and co-cultured with 3LL-OVA cells, which express cytosolic ovalbumin. A higher cytotoxicity against 3LL-OVA cells was displayed by OT-1 CTLs (Fig. 4A). Next, we detected the distribution of GSDMD in CTL-target cell conjugates. As shown in Fig. 4B, CTLs engaged in cognate interactions with 3LL-OVA cells displayed a significant enrichment of GSDMD toward the lytic synapse. Moreover, colocalization of GSDMD with granzyme B was observed in the proximity of the lytic synapse (Fig. 4B). Further, shRNAs were used to knockdown the expression of GSDMD in $CD8^+$ T cells by transfection, prior to use in functional assays. ShGsdmd-1 and shGsdmd-2 depleted GSDMD expression by 65.82 ± 7.63% and 69.38 ± 7.28% in the OT-1 T cells (Fig. 4C). We found that shRNAs to GSDMD significantly decreased CTL-mediated cytolysis of 3LL-OVA targets compared with that with control scrambled shRNA (Fig. 4D), which implied an important role for GSDMD in CTL cytotoxicity.

3.5. GSDMD deficiency reduces the cytolytic capacity of human $CD8^+$ T lymphocytes

To investigate whether GSDMD also plays an important role in human $CD8^+$ T cell cytotoxicity, we initially examined T cell responses to lung cancer cells. Peripheral blood mononuclear cells (PBMCs) were isolated from the blood of patients with LUAD. T cells were stimulated with soluble anti-CD3/anti-CD28 in RPMI 1640 medium supplemented with 10% fetal bovine serum (FBS). After 7 days, $CD8^+$ T cells were purified by negative selection and added to cultured lung cancer cells. Among the cancer cell lines screened, we found that H1299 cells were efficiently killed and showed the highest sensitivity to *ex-vivo* expanded T cells (Fig. 5A). Next, we analyzed the distribution of GSDMD in T cells that encountered H1299 cells. The results showed that the GSDMD protein was enriched around the lytic synapse and co-localized with granzyme B (Fig. 5B). Further, shRNAs were used to knockdown the expression of GSDMD in CD8+ T cells by transfection, prior to use in functional assays. ShGsdmd-1 and shGsdmd-2 depleted GSDMD expression by 60.02 ± 4.79% and 65.08 ± 7.63% in the human T cells (Fig. 5C). We found that GSDMD-deficient T cells displayed decreased killing activity (Fig. 5D), consistent with the results obtained from OT-1 T cells. All the above results indicated that GSDMD is required for $CD8^+$ T cell cytotoxicity.

4. Discussion

In 2015, two independent groups used genomic screening techniques to identify GSDMD as a substrate of inflammasome associated caspases, which upon cleavage generates an effector domain that induces pores in the cell membrane leading to pyroptosis [22,23]. Recently, many non-pyroptotic functions for GSDMD were found. Evavold CL et al. found that GSDMD pores represent conduits for the secretion of cytosolic cytokines under conditions of macrophages hyperactivation [27]. Banerjee I et al. found GSDMD activated by the Aim2

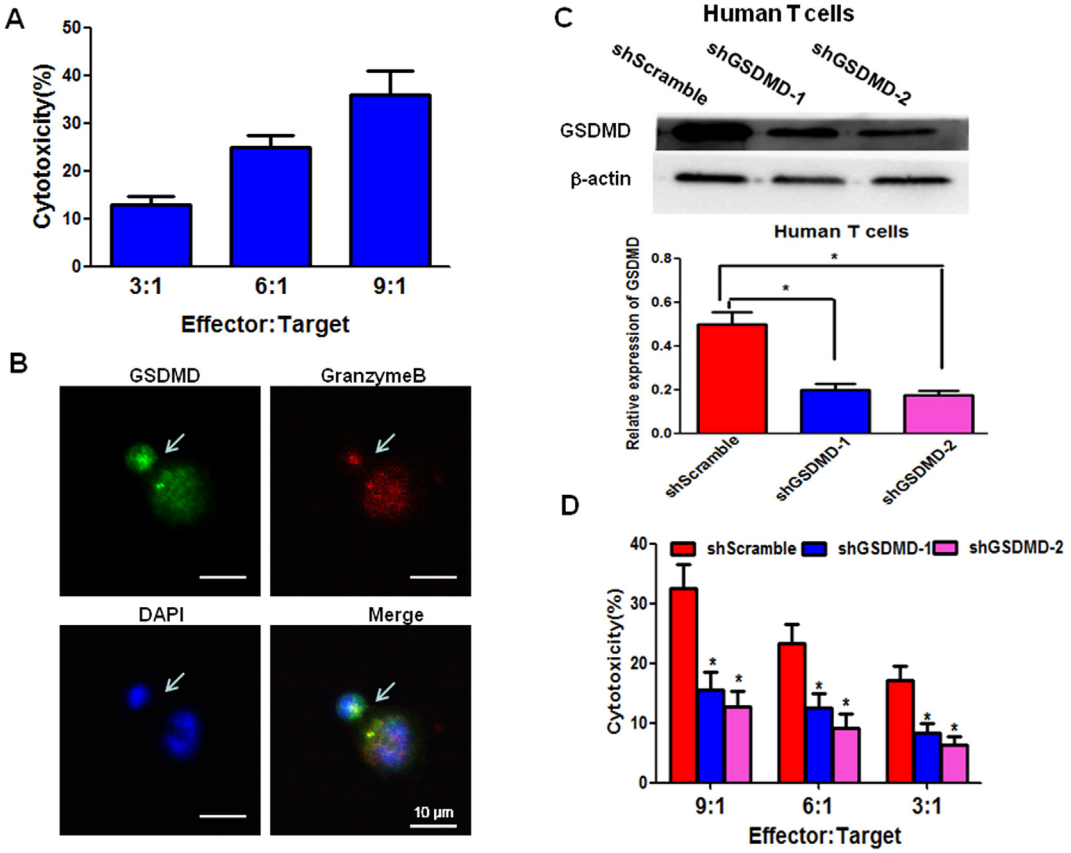

Fig. 5. GSDMD deficiency reduces the cytolytic capacity of human CD8$^+$ T cells. (A) Activated CD8$^+$ T cell cytotoxicity on H1299 target cells. CD8$^+$ T cells stimulated with 5 μg/ml of soluble anti-CD3 and anti-CD28 for 7 days were co-cultured with H1299 at different ratios. After 4 h, the supernatant was collected, and the cytolysis efficiency was calculated according to the release of LDH into the supernatant. (B) Fluorescence microscopy images of activated CD8$^+$ T cells conjugated with H1299 cells. Activated CD8$^+$ T cells were mixed with H1299 cells for 4 h, fixed, and stained for GSDMD and granzymeB to visualize the distribution of GSDMD and granzymeB in the human activated CD8$^+$ T cells. (C) ShRNA-mediated suppression of GSDMD was routinely confirmed by Western blot. (D) Percentage lysis of H1299 target cells by activated CD8$^+$ T cells expressing scrambled or GSDMD shRNA at different effector to target ratios. All killing assays were performed in triplicates. *P $<$ 0.05.

inflammasome suppressed cGAS-driven type I interferon response to cytosolic DNA and Francisella novicida in a pyroptosis-independent manner in macrophages [28]. Here, we report an additional biological role for GSDMD in CTL-mediated cytotoxicity.

CTLs principally eliminate cancer cells by releasing the contents of cytotoxic granules into the immune synapse formed with their target cell [29]. The granule serine proteases, known as Gzms, induce apoptosis after they are delivered into the target cell cytoplasm by perforin [30]. However, cell lysis may be the real nature of CTL-mediated cell death, as determined by chromium-51 or LDH release assays. Thus far, there has been no reasonable explanation for this paradoxical phenomenon. It is tempting to speculate that other pore-forming proteins are associated with CTL-mediated cell killing. Given that GSDMD can only cause cell lysis from within mammalian cells because of the asymmetric distribution of phosphoinositides on the plasma membrane [19], GSDMD may be delivered into the target cells along with granzyme B and cause cell swelling and eventual lysis. Our results obtained using bioinformatics supported the hypothesis that GSDMD was associated with CTL function since GSDMD consistently correlated with CTL markers in the tumor samples from TCGA.

The GSDM family shares approximately 45% sequence homology, with the gasdermin-N domain being the most conserved region [31,32]. The gasdermin-N domains of GSDMA/GSDMA3, GSDMB, GSDMC, and DFNA5 all can form pores and induce mammalian cell pyroptosis [19,32]. Therefore, we asked whether other GSDM family genes may play a role in CTL function. Although GSDMA positively correlated with CD8$^+$ T cell markers in LUAD, and GSDMB correlated with CD8$^+$ T cell markers in the melanoma cohorts, only GSDMD positively correlated with CD8$^+$ T cell markers in all cohorts. Furthermore, the mRNA expression level of GSDMD was the highest among GSDM family genes in OT-1 CD8$^+$ T cells. The expression of GSDMD was also high in human CD8$^+$ T cells. Therefore, we concluded that GSDMD, but not other genes in the GSDM family, play a critical role in CTL function.

Next, we determined the state of GSDMD in naïve and activated CD8$^+$ T cells. Previous reports showed that GSDMD, as the executioner of pyroptosis, is cleaved upon induction of pyroptosis in monocytes [22]. In the present study, the cleavage of GSDMD in CD8$^+$ T cells was investigated for the first time. We found that GSDMD, mainly in the cleaved form, was up-regulated in OT-1 CTLs activated with $OVA_{257–264}$ and activated human CD8$^+$ T cells, along with other effector function molecules, such as perforin-1 and granzyme B. All these data suggested that GSDMD expressed in activated CD8$^+$ T cells was mainly in an active form. Why does the N-terminal domain of GSDMD not bind to the membrane in the activated CD8$^+$ T cells. We speculated that cleaved GSDMD-N domain may be bound by GSDMD-C domain and the activity of GSDMD-N was inhibited by this binding. Once GSDMD-N domain was delivered into the target cells, GSDMD-N domain may be liberated from GSDMD-C domain by a unknown mechanism. Then the GSDMD–N domain can bind to the target cell membrane and induce target cell death. GSDMD-N domain was not able to interact with the outer plasma membrane of cells, preventing unwarranted cell death and tissue damage.

How GSDMD cleavage occurs in CTLs remains unclear. Recently, the crystal structure of GSDMD was obtained from molecular modeling

based on the crystal structure of GSDMA3. The overall structure was separated into gasdermin-N and gasdermin-C domains, with a long loop harboring the inflammatory caspase cleavage site. Full-length GSDMD is inactive because of binding of the gasdermin-C domain to the gasdermin-N domain in an auto-inhibitory fashion [19]. Upon induction of pyroptosis, GSDMD is cleaved by inflammatory caspases at the conserved residue D276, which separates GSDMD into GSDMD-N and GSDMD-C domains. The inflammatory caspases comprise caspase-1, -4, -5 and 11 [33], and we tested whether these caspases were activated in activated $CD8^+$ T cells. Our results demonstrated that caspase-11 in mouse $CD8^+$ T cells and caspase-4 in human $CD8^+$ T cells were activated during the activation of primary T cell. Moreover, T cell activation-induced GSDMD cleavage was attenuated by a pan-caspase inhibitor zVAD-FMK or shRNA targeting caspase-11 or caspase-4. These results suggested that GSDMD cleavage was attributed to the inflammatory action of caspase-4 or -11 in activated T cells. How caspase-4 or -11 was activated remains unclear. Apart from caspase-4 and -11, caspase-3 and -8 were also activated in newly activated T cells without an apoptotic phenotype [34]. Because granzyme B activates members of the caspase family [35], we speculate that up-regulated granzyme B may accounts for the activation of caspase-4 and -11 in activated $CD8^+$ T cells.

Although we found that GSDMD cleavage was increased in the cytolytic T lymphocytes, its role in the effector function of CTLs is not clear. To examine this, we initially assessed colocalization between GSDMD and granzyme B in CTLs conjugated with target cells. We found that GSDMD co-localized with granzyme B in the vesicles which polarized toward the immune synapse. In addition, we assessed GSDMD-knockdown CTLs for their cytotoxic function and found reduced levels of target cell killing compared with control CTLs, which suggests that GSDMD contributes to CTL-mediated killing.

In summary, the results presented here identify a previously unknown role of GSDMD in CTLs and demonstrate that GSDMD is required for an optimal CTL response to cancer cells. According to our present study, we propose a new hypothesis that pore-forming proteins, which can form pores from within mammalian cells, are delivered into the target cell and induce cytolysis.

Supplementary data to this article can be found online at https://doi.org/10.1016/j.intimp.2019.105713.

Authors' contributions

MX and YS performed the concept and design of experiments, analysis and interpretation of the data and manuscript preparation. MX, WG, BW and PZ performed the study. FL gives valuable advice in this study. All authors read and approved the final manuscript.

Declaration of Competing Interest

The authors report no conflicts of interest related to this work.

References

[1] L. Chávez-Galán, A.M.C. Arenas-Del, E. Zenteno, R. Chávez, R. Lascurain, Cell death mechanisms induced by cytotoxic lymphocytes, Cell. Mol. Immunol. 6 (1) (2009) 15–25.

[2] I. Voskoboinik, J.C. Whisstock, J.A. Trapani, Perforin and granzymes: function, dysfunction and human pathology, Nat. Rev. Immunol. 15 (6) (2015) 388–400.

[3] B. Lowin, M. Hahne, C. Mattmann, J. Tschopp, Cytolytic T-cell cytotoxicity is mediated through perforin and Fas lytic pathways, Nature 370 (6491) (1994) 650–652.

[4] P.J. Peters, J. Borst, V. Oorschot, M. Fukuda, O. Krähenbühl, J. Tschopp, et al., Cytotoxic T lymphocyte granules are secretory lysosomes, containing both perforin and granzymes, J. Exp. Med. 173 (5) (1991) 1099–1109.

[5] G. de Saint Basile, G. Ménasché, A. Fischer, Molecular mechanisms of biogenesis and exocytosis of cytotoxic granules, Nat. Rev. Immunol. 10 (8) (2010) 568–579.

[6] J.W. Heusel, R.L. Wesselschmidt, S. Shresta, J.H. Russell, T.J. Ley, Cytotoxic lymphocytes require granzyme B for the rapid induction of DNA fragmentation and apoptosis in allogeneic target cells, Cell 76 (6) (1994) 977–987.

[7] L. Shi, C.M. Kam, J.C. Powers, R. Aebersold, A.H. Greenberg, Purification of three cytotoxic lymphocyte granule serine proteases that induce apoptosis through distinct substrate and target cell interactions, J. Exp. Med. 176 (6) (1992) 1521–1529.

[8] L. Shi, S. Mai, S. Israels, K. Browne, J.A. Trapani, A.H. Greenberg, Granzyme B (GraB) autonomously crosses the cell membrane and perforin initiates apoptosis and GraB nuclear localization, J. Exp. Med. 185 (5) (1997) 855–866.

[9] J.A. Trapani, M.J. Smyth, Functional significance of the perforin/granzyme cell death pathway, Nat. Rev. Immunol. 2 (10) (2002) 735–747.

[10] W. Boyle, An extension of the 51Cr-release assay for the estimation of mouse cytotoxins, Transplantation 6 (6) (1968) 761–764.

[11] K.R. Jerome, D.D. Sloan, M. Aubert, Measurement of CTL-induced cytotoxicity: the caspase 3 assay, Apoptosis 8 (6) (2003) 563–571.

[12] M.A. Karimi, E. Lee, M.H. Bachmann, A.M. Salicioni, E.M. Behrens, T. Kambayashi, et al., Measuring cytotoxicity by bioluminescence imaging outperforms the standard chromium-51 release assay, PLoS One 9 (2) (2014) e89357.

[13] J.E. Goldberg, S.W. Sherwood, C. Clayberger, A novel method for measuring CTL and NK cell-mediated cytotoxicity using annexin V and two-color flow cytometry, J. Immunol. Methods 224 (1–2) (1999) 1–9.

[14] J.D. Young, H. Hengartner, E.R. Podack, Z.A. Cohn, Purification and characterization of a cytolytic pore-forming protein from granules of cloned lymphocytes with natural killer activity, Cell 44 (6) (1986) 849–859.

[15] J. Thiery, D. Keefe, S. Boulant, E. Boucrot, M. Walch, D. Martinvalet, et al., Perforin pores in the endosomal membrane trigger the release of endocytosed granzyme B into the cytosol of target cells, Nat. Immunol. 12 (8) (2011) 770–777.

[16] P. Bolitho, I. Voskoboinik, J.A. Trapani, M.J. Smyth, Apoptosis induced by the lymphocyte effector molecule perforin, Curr. Opin. Immunol. 19 (3) (2007) 339–347.

[17] D. Keefe, L. Shi, S. Feske, R. Massol, F. Navarro, T. Kirchhausen, et al., Perforin triggers a plasma membrane-repair response that facilitates CTL induction of apoptosis, Immunity 23 (3) (2005) 249–262.

[18] J.A. Lopez, O. Susanto, M.R. Jenkins, N. Lukoyanova, V.R. Sutton, R.H. Law, et al., Perforin forms transient pores on the target cell plasma membrane to facilitate rapid access of granzymes during killer cell attack, Blood 121 (14) (2013) 2659–2668.

[19] J. Ding, K. Wang, W. Liu, Y. She, Q. Sun, J. Shi, et al., Pore-forming activity and structural autoinhibition of the gasdermin family, Nature 535 (7610) (2016) 111–116.

[20] N. Saeki, T. Usui, K. Aoyagi, D.H. Kim, M. Sato, T. Mabuchi, et al., Distinctive expression and function of four GSDM family genes (GSDMA-D) in normal and malignant upper gastrointestinal epithelium, Genes Chromosom. Cancer 48 (3) (2009) 261–271.

[21] W.T. He, H. Wan, L. Hu, P. Chen, X. Wang, Z. Huang, et al., Gasdermin D is an executor of pyroptosis and required for interleukin-1β secretion, Cell Res. 25 (12) (2015) 1285–1298.

[22] J. Shi, Y. Zhao, K. Wang, X. Shi, Y. Wang, H. Huang, et al., Cleavage of GSDMD by inflammatory caspases determines pyroptotic cell death, Nature 526 (7575) (2015) 660–665.

[23] N. Kayagaki, I.B. Stowe, B.L. Lee, K. O'Rourke, K. Anderson, S. Warming, et al., Caspase-11 cleaves gasdermin D for non-canonical inflammasome signalling, Nature 526 (7575) (2015) 666–671.

[24] X. Liu, Z. Zhang, J. Ruan, Y. Pan, V.G. Magupalli, H. Wu, et al., Inflammasome-activated gasdermin D causes pyroptosis by forming membrane pores, Nature 535 (7610) (2016) 153–158.

[25] M. de la Roche, A.T. Ritter, K.L. Angus, C. Dinsmore, C.H. Earnshaw, J.F. Reiter, et al., Hedgehog signaling controls T cell killing at the immunological synapse, Science 342 (6163) (2013) 1247–1250.

[26] S. Feng, D. Fox, S.M. Man, Mechanisms of gasdermin family members in inflammasome signaling and cell death, J. Mol. Biol. 430 (18 Pt B) (2018) 3068–3080.

[27] C.L. Evavold, J. Ruan, Y. Tan, S. Xia, H. Wu, J.C. Kagan, The pore-forming protein gasdermin D regulates interleukin-1 secretion from living macrophages, Immunity 48 (1) (2018) 35–44.e6.

[28] I. Banerjee, B. Behl, M. Mendonca, G. Shrivastava, A.J. Russo, A. Menoret, et al., Gasdermin D restrains type I interferon response to cytosolic DNA by disrupting ionic homeostasis, Immunity 49 (3) (2018) 413–426.e5.

[29] A. Grakoui, S.K. Bromley, C. Sumen, M.M. Davis, A.S. Shaw, P.M. Allen, et al., The immunological synapse: a molecular machine controlling T cell activation, Science 285 (5425) (1999) 221–227.

[30] D.A. Anthony, D.M. Andrews, S.V. Watt, J.A. Trapani, M.J. Smyth, Functional dissection of the granzyme family: cell death and inflammation, Immunol. Rev. 235 (1) (2010) 73–92.

[31] M.M. Gaidt, V. Hornung, Pore formation by GSDMD is the effector mechanism of pyroptosis, EMBO J. 35 (20) (2016) 2167–2169.

[32] J. Shi, W. Gao, F. Shao, Pyroptosis: gasdermin-mediated programmed necrotic cell death, Trends Biochem. Sci. 42 (4) (2017) 245–254.

[33] O. Julien, J.A. Wells, Caspases and their substrates, Cell Death Differ, 2017.

[34] T. Rajah, S.C. Chow, The inhibition of human T cell proliferation by the caspase inhibitor z-VAD-FMK is mediated through oxidative stress, Toxicol. Appl. Pharmacol. 278 (2) (2014) 100–106.

[35] V.R. Sutton, J.A. Trapani, Proteases in lymphocyte killer function: redundancy, polymorphism and questions remaining, Biol. Chem. 391 (8) (2010) 873–879.